

# Structured mixing model for stirred bioreactors: An extension to the stochastic approach

F. Delvigne<sup>a,\*</sup>, J. Destain<sup>a</sup>, P. Thonart<sup>a,b,1</sup>

<sup>a</sup> Centre Wallon de Biologie Industrielle, Unité de Bio-industries, Faculté des Sciences Agronomiques de Gembloux,  
Passage des déportés, 2, B-5030 Gembloux, Belgium

<sup>b</sup> Centre Wallon de Biologie Industrielle, Service de Technologie Microbienne, Université de Liège, Sart-Tilman, B40, B-4000 Liège, Belgium

Received 20 January 2005; received in revised form 14 June 2005; accepted 28 June 2005

## Abstract

The potentiality of a stochastic approach is examined in the case of a mixing model for stirred vessels. This model is interesting due to the probabilistic and discrete properties that can be used further to facilitate the implementation of a hydrodynamic model into complex reacting systems, such as those encountered in bioprocesses. Stochastic model performances are compared to well known deterministic compartment mixing models (CM). It appears that parameters coming from CM can be used in the stochastic approach and that they give equivalent results. A methodology is elaborated that simplifies the determination procedure of the adjustable parameters of the stochastic model. The most important parameter to determine is the time step of a simulation performed by the aim of the stochastic model. Indeed, the time step is not explicitly given by the model and a correlation is necessary to translate simulation intervals into real time increments. After an appropriate analysis of several mixing systems (single or multi-agitated), it appears that a simple correlation involving circulation time could be used to perform this translation. The correlation contains an adjustable parameter, which has been quantified for the operating conditions covered in the study. The circulation of micro-organisms was also simulated simply by using the transition matrix coming from the stochastic model, which shows the potentiality of this kind of model in the field of complex reacting systems, such as those encountered in bioprocesses.

© 2005 Elsevier B.V. All rights reserved.

**Keywords:** Structured mixing model; Stochastic approach; Compartment model

## 1. Introduction

The elaboration of a probabilistic mixing model from the well known structure of a compartment model (CM) has been investigated in this study. CM has been widely described in the literature and allows the representation of mixing phenomena with a relatively good resolution (depending on the model structure). Nevertheless, only a few number of compartment models have been applied to the description of mixing problems in bioprocesses [1–3].

The idea is to extend this kind of model to a stochastic approach in which the passage of particles from one flow region to another is governed by probabilities. Interest in

this kind of model comes from its probabilistic and discrete properties, which facilitate implementation with complex reacting systems, such as fermentation processes. In addition, the stochastic model is very simple to compute and does not require large computation space or time. This low computational requirement is an additional reason allowing the inclusion of this model within more complex ones, such as microbial kinetic models.

In order to understand the working principles of these models, a short literature review is necessary. As stated previously, a large number of compartment mixing models are available in the literature. The first structures were very simple and comprised a single compartment per agitation stage, a compartment corresponding to a volume element of the reactor considered to be perfectly mixed [4–10]. The structures then evolved and were applied to stirred bioreactors. This led to very complex model structures, such as the

\* Corresponding author. Tel.: +32 81 62 23 11; fax: +32 81 61 42 22.

E-mail address: delvigne.f@fsagx.ac.be (F. Delvigne).

<sup>1</sup> Tel.: +32 43 66 28 61; fax: +32 43 66 28 62.

### Nomenclature

$c$	correlating factor for the determination of the transition time interval
CM	compartment model
$d$	impeller diameter (m)
$D$	stirred vessel diameter (m)
$k$	number of transitions that are necessary to reach homogeneity
$n$	number of transitions before all states are visited by tracer particles
$n_{loop}$	number of circulation loops in a two-dimensional CM
$N$	stirrer speed ( $s^{-1}$ )
$N_{qc}$	circulation or flow number (dimensionless)
NOZ	network-of-zones
$q_c$	circulation flow rate per loop in the CM ( $m^3/s$ )
$q_e$	turbulent flow rate ( $m^3/s$ )
$q_t$	tangential flow rate ( $m^3/s$ )
$q_{exit}$	evacuation flow rate used in RTD experiments ( $m^3/s$ )
$Q_c$	circulation flow rate ( $m^3/s$ )
RTD	residence time distribution
$S$	state vector
$S_0$	initial state vector
$S_i$	state vector after $i$ th transition
$t_c$	circulation time (s)
$t_m$	mixing time (s)
$T$	transition matrix

network-of-zones (NOZ), which comprises a large number of interconnected compartments [11,12]. These NOZ models have a higher resolution but require more computation space because of the large number of differential equations involved.

In terms of similarity, the compartment network of a classical CM can be used in a stochastic context. Indeed, this model consists of several states that can be assimilated into the compartments of the CM. The structures are therefore very similar and differences between the two approaches come from the mathematical formulation of the models. Stochastic mathematical expression does not involve ordinary differential equations, but a transition probability matrix that orientates the evolution of the system. This system comprises several states that correspond in our application to the concentrations in several delimited zones in the stirred vessel. The CM principle, having been greatly improved upon, is useful to take as a basis from which to elaborate stochastic models that are not widely applied in the area of fluid mixing, except in the case of some theoretical considerations [13–15]. Of interest is the fact that stochastic models have properties that can be used to study special mixing phenomena, which are important, notably in bioprocesses.

The first property is the stochastic aspect of the model that can be used to make particle following studies [14]. This aspect is very important in bioprocesses because it enables the easy description of circulation paths taken by microorganisms inside a stirred bioreactor, and allows the determination of, for example, the frequency at which microbes are exposed to high nutrient concentrations or high shear stress [2,16]. Circulation simulation will be investigated in the last section of this paper.

The second property is the discrete aspect of the model that can be interesting when coupling hydrodynamics with complex reactions, such as microbial kinetics [17]. This property will be investigated in further studies. There are many other properties that can be usefully exploited. One example is the absorbing property, which will be investigated in this study.

## 2. Material and methods

### 2.1. Experimental stirred vessel

Two impellers were used: rushton disk turbines (RDT6) and lightning hydrofoils A315 (pumping downward), both having a diameter of 0.1 m. Some combinations were particularly investigated: RDT6–RDT6, RDT6–A315 (the first cited impeller was placed at the lower part of the vessel and the second one at the upper part; impeller clearance from the bottom of the vessel: 0.1 m; inter-impeller clearance: 0.2 m). Photographs of these impellers are shown in Fig. 2. All experiments were performed in a Perspex stirred vessel ( $D=0.22$  m) equipped with four baffles.

### 2.2. Mixing time experiments

Three kinds of mixing experiments were employed in this study, each kind permitting the investigation of a specific aspect of mixing behaviour.

The first kind of experiment consisted of measuring the mixing time in a vertical plane of the stirred vessel. To achieve this, a series of thermocouples attached onto a baffle of the vessel were used. The small dimension of these probes (0.45 mm diameter) allows the control of only a restricted volume element in the vessel. It can thus be assumed that only a vertical plane in the vessel was involved in the experiments facilitating the implementation of the results in a CM.

The second kind of experiment was also a mixing time measurement, but here we used conductivity probes. In this case, due to the larger dimensions of the probes (1 cm diameter), the volume elements are bigger and must be considered in a three-dimensional context. Experiments conducted in this way were used to implement three-dimensional models. The positions of the probes for these two kinds of experiment are presented in Fig. 1.

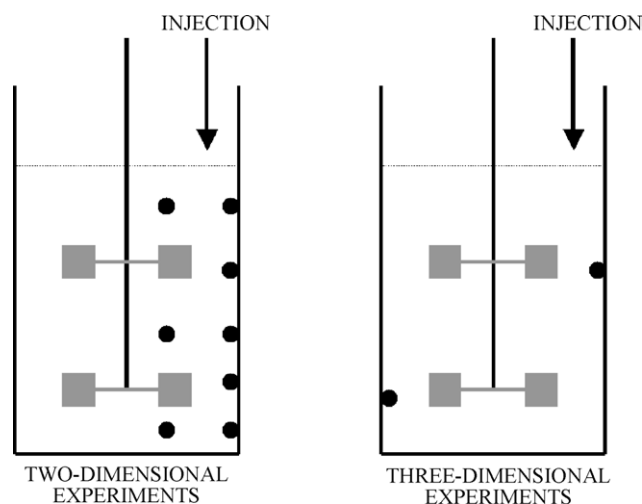


Fig. 1. Locations of thermosensors (left) and conductivity probes (right) in the stirred vessel.

The third kind of experiment was a residence time distribution (RTD) measurement. The apparatus is the same as for the previous one, but here fluid is continuously fed and extracted from the vessel at a flow rate of 50 ml/s. Conductivity probes allow the on-line measurement of the decreasing concentration of the injected tracer. These experiments allowed for an improvement of the stochastic model, by analysing the absorbing state property.

For the first and second kinds of experiments, the mixing time (corresponding to a degree of mixing of 85%) was calculated from tracer curves using the method presented by Mayr et al. [18]. In this method, an ideal response function corresponding to the tracer curve of a pulse added in a perfectly mixed reactor must be first determined. The standard deviations of each experimental tracer curve (5 or 8 for the thermal method and 1 or 2 for the conductivity method) from this ideal response function are then calculated. The standard deviations are summed and divided by the number of sensors to give an inhomogeneity function varying from 0 (total homogeneity) to 1 (total inhomogeneity). In this study, the mixing time corresponded to the time at which the value of the inhomogeneity function dropped to 0.15, or in other words a degree of mixing of 85%. The inhomogeneity degree was chosen at a high enough level to make the fluctuation signal of the probes negligible.

A large amount of data were collected in this way and were used to elaborate a mixing database containing the experimental conditions, the mixing time results and the parameter estimation for each model. In order to limit the experimental field and to concentrate our attention on stochastic model development, only the results performed in water in non-aerated conditions will be considered in this paper. Indeed, aeration and viscosity led to a modification of the parameters of the model (e.g., circulation flow drop with increasing aeration and/or viscosity). This requires extensive discussion, which cannot be included in the space allowed.

### 2.3. Mathematical models: CM and stochastic approaches

The aim of this paper is to translate compartment mixing model knowledge into a stochastic context. Advantages of such an approach have been briefly discussed in Section 1 and will be reviewed at the end of this study.

It is of practical importance to begin with a brief description of the two models presented here and to discuss their differences. In the case of the compartment mixing (CM) approach, the flows between the interconnected compartments are responsible for homogenisation. In the case of a stochastic model, it is a series of probabilistic transitions between states that are responsible for the repartition of the tracer in the whole vessel. The CM approach consists of a set of ordinary differential equations (one for each compartment), which are resolved in a continuous manner with an appropriate numerical method (in our case, a Runge–Kutta routine was used). More details about CM construction can be found in [6,11]. The stochastic model consists of an initial state vector  $S_0$ , which is multiplied with a transition matrix  $T$  to give a new state,  $S_1$ . This procedure can be represented by the following equation:

$$\text{For the first transition : } S_1 = T \cdot S_0 \quad (1)$$

The next step involves the multiplication of the new state vector  $S_1$  with the same transition matrix  $T$  until a steady state is reached:

$$\text{For the second transition : } S_2 = T \cdot S_1 \quad \text{or} \quad S_2 = T^2 \cdot S_0 \quad (2)$$

$$\text{For the } i\text{th transition : } S_i = T \cdot S_{i-1} \quad \text{or} \quad S_i = T^i \cdot S_0 \quad (3)$$

In our case, the state vector contained the tracer concentrations for all states, a state corresponding to a region of the agitated vessel (or a compartment in the CM context).

The numerical implementation of a stochastic simulation is thus very simple because it involves only matrix multiplication. An important fact is that the stochastic model is a discrete-space and discrete-time model, whereas CM is a continuous-time and discrete-space model. It thus appears that the two models work on a very different basis. The dissimilarities between the CM and the stochastic mixing models need to be analysed in order to facilitate the translation of knowledge between the two approaches.

In order to stay within the same referential for all the models constructed in this paper, the number of compartments per agitation stage was always 8. This is the minimum number of compartments that allow for differentiation between axial and radial impellers.

The impellers used (RDT6 and A315) exhibit three different flow patterns that influence the orientation of the circulation flow rates in the CM model. RDT6 exhibits a radial flow pattern and, on the opposite, hydrofoil A315 has an axial

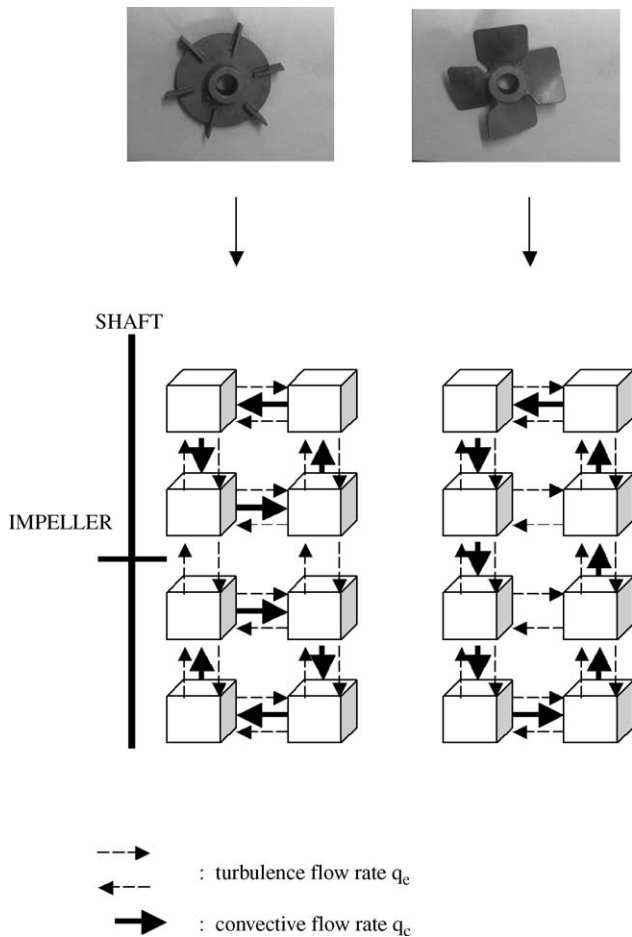


Fig. 2. “Basic plane” compartment network for a radial impeller (RDT6 on the left) and an axial impeller (A315 on the right).

flow pattern. The “basic plane” models for each impeller are presented in Fig. 2.

These basic structures can be combined to model a multi-staged vessel. In the case of a three-dimensional model, eight basic plane structures are arranged in series for an agitation stage, these planes being linked to each other by a tangential flow rate  $q_t$  (Fig. 3).

The first step in this study was the estimation of the parameter  $q_e$  of the CM model. This allowed the determination of the ratio  $q_c/q_e$ , which would then be used for the qualitative analysis of the stochastic model. The translation from the CM model to the stochastic context is illustrated in Fig. 4. This figure represents the global structure of the two models.

The ratio  $q_c/q_e$  coming from the CM model was used to calculate the probabilities of shifting from one state to another in the stochastic model. These probabilities were collected in the transition matrix  $T$ . An example of a transition matrix valid for a RDT6 system is given in Fig. 5.

The ratio  $q_c/q_e$  only has an impact on the shape of the tracer curves and governs only the qualitative aspect of the results. The quantitative aspect is taken into account by fixing the time required to achieve a transition when running a simulation

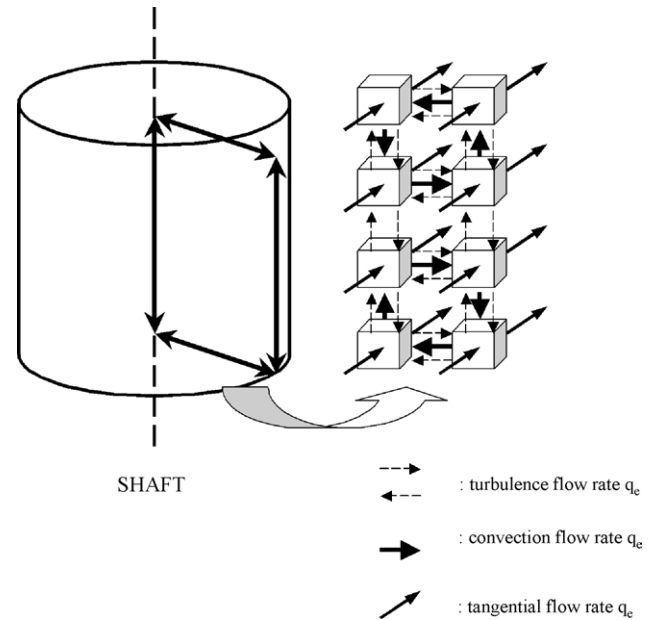


Fig. 3. Arrangement scheme of “basic plane” structures to give a three-dimensional compartment model.

with the stochastic model. This aspect will be analysed in detail in Section 3.

#### 2.4. Parameter estimation procedure

For the two-dimensional compartment model, there are two adjustable parameters:  $q_e$  and  $q_c$ . The circulation flow rate  $q_c$  was calculated by the use of the following equation coming from dimensional analysis [3]:

$$q_c = \frac{N_{q_c} \cdot N \cdot d^3}{n_{\text{loop}}} \quad (4)$$

with  $n_{\text{loop}}$  being the number of circulation loops implemented by the model ( $n_{\text{loop}}=2$  for the RDT6 and  $n_{\text{loop}}=1$  for the A315 impeller).  $N_{q_c}$  is a dimensionless circulation number that depends only on the impeller geometry in the turbulent flow regime ( $N_{q_c} = 1.51$  for RDT6;  $N_{q_c} = 1.3$  for A315).

The turbulence flow rate  $q_e$  was estimated by sensitivity analysis. For a calculated value of  $q_c$ , the value of  $q_e$  was modulated to match the measured mixing time. The maximum and the minimum values of  $q_e$  matching with the experimental mixing time were determined, the mean corresponding to the used value of  $q_e$  in the simulations.

For the three-dimensional versions (Fig. 3), there was an additional parameter to determine: the tangential flow rate  $q_t$ . The determination of this parameter will be discussed in the following sections.

After parameter determination of the CM model, all the flow rates  $q_c$ ,  $q_e$  and  $q_t$  were collected to calculate the transition matrix  $T$  of the corresponding stochastic models ( $q_c$  and  $q_e$  for the two-dimensional versions;  $q_c$ ,  $q_e$  and  $q_t$  for the three-dimensional versions).

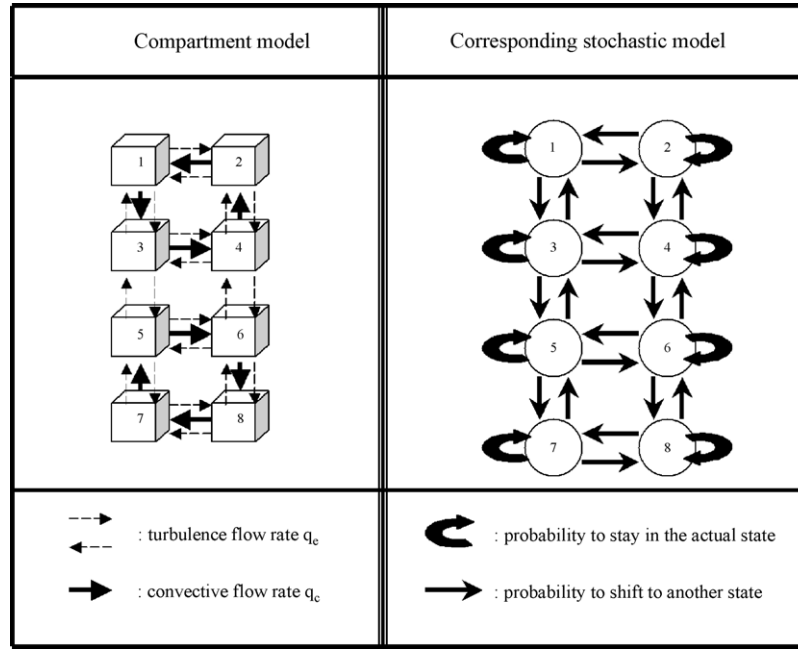


Fig. 4. Comparison of the compartment model and stochastic approach.

	$S_1$	$S_2$	$S_3$	$S_4$	$S_5$	$S_6$	$S_7$	$S_8$
$S_1$	$\frac{2q_e}{4q_e + q_c}$	$\frac{q_e}{4q_e + q_c}$	$\frac{q_e + q_c}{4q_e + q_c}$	0	0	0	0	0
$S_2$	$\frac{q_e + q_c}{4q_e + q_c}$	$\frac{2q_e}{4q_e + q_c}$	0	$\frac{q_e}{4q_e + q_c}$	0	0	0	0
$S_3$	$\frac{q_e}{6q_e + q_c}$	0	$\frac{3q_e}{6q_e + q_c}$	$\frac{q_e + q_c}{6q_e + q_c}$	$\frac{q_e}{6q_e + q_c}$	0	0	0
$S_4$	0	$\frac{q_e + q_c}{6q_e + q_c}$	$\frac{q_e}{6q_e + q_c}$	$\frac{3q_e}{6q_e + q_c}$	0	$\frac{q_e}{6q_e + q_c}$	0	0
$S_5$	0	0	$\frac{q_e}{6q_e + q_c}$	0	$\frac{3q_e}{6q_e + q_c}$	$\frac{q_e + q_c}{6q_e + q_c}$	$\frac{q_e}{6q_e + q_c}$	0
$S_6$	0	0	0	$\frac{q_e}{6q_e + q_c}$	$\frac{q_e}{6q_e + q_c}$	$\frac{3q_e}{6q_e + q_c}$	0	$\frac{q_e + q_c}{6q_e + q_c}$
$S_7$	0	0	0	0	$\frac{q_e + q_c}{4q_e + q_c}$	0	$\frac{2q_e}{4q_e + q_c}$	$\frac{q_e}{4q_e + q_c}$
$S_8$	0	0	0	0	0	$\frac{q_e}{4q_e + q_c}$	$\frac{q_e + q_c}{4q_e + q_c}$	$\frac{2q_e}{4q_e + q_c}$

Fig. 5. Example of transition matrix corresponding to the stochastic model presented in Fig. 4 (right-hand side).

### 3. Results and discussion

#### 3.1. Two-dimensional mixing time experiments

As previously discussed, the compartment model has two adjustable parameters. The circulation flow rate  $q_c$  was calculated with the dimensional equation (4). The turbulent flow rate was estimated by the procedure outlined in Section 2. All the results concerning these two parameters are presented in Table 1.

Fig. 6 shows a comparison between experimental results and a compartment model simulation for the mixing of tracer pulse poured at the top of the vessel.

Adjustable parameters were calculated according to the method discussed in Section 2. The mixing times given by the

model matched the experimental ones exactly, but the shape of tracer curves recorded by the probes at different locations in a vertical plane of the vessel did not exactly match with the simulation results. Nevertheless, simulated tracer curves presented the same tendencies as the real ones (e.g., the tracer curves recorded near the pulse location exhibited a strong peak, which was not observed for the lower locations in the vessel).

There are two principal factors affecting the quality of the simulation. First, the number of compartments considered. If the number increases, the resolution of the model will be higher and tracer curves may be more differentiated. A high resolution can be obtained with models containing a large number of compartments with several parallel circulation loops. Such models are called network-of-zones.

Table 1

Estimation of the adjustable parameters of the compartment model for each impeller system investigated

Impeller(s)	$N$ ( $\text{min}^{-1}$ )	Calculated $q_c$ ( $\text{m}^3/\text{s}$ )		Estimated $q_e$ ( $\text{m}^3/\text{s}$ )
		Lower stage	Upper stage	
RDT6	230	0.0028	–	0.0155
RDT6	270	0.0033	–	0.0205
RDT6	360	0.0045	–	0.0295
RDT6	450	0.0056	–	0.029
RDT6–RDT6	230	0.0028	0.0028	0.04
RDT6–RDT6	270	0.0033	0.0033	0.0475
RDT6–RDT6	360	0.0045	0.0045	0.0645
RDT6–RDT6	450	0.0056	0.0056	0.0725
RDT6–A315	230	0.0028	0.0049	0.084
RDT6–A315	270	0.0033	0.0058	0.123
RDT6–A315	360	0.0045	0.0078	0.122
RDT6–A315	450	0.0056	0.0097	0.158



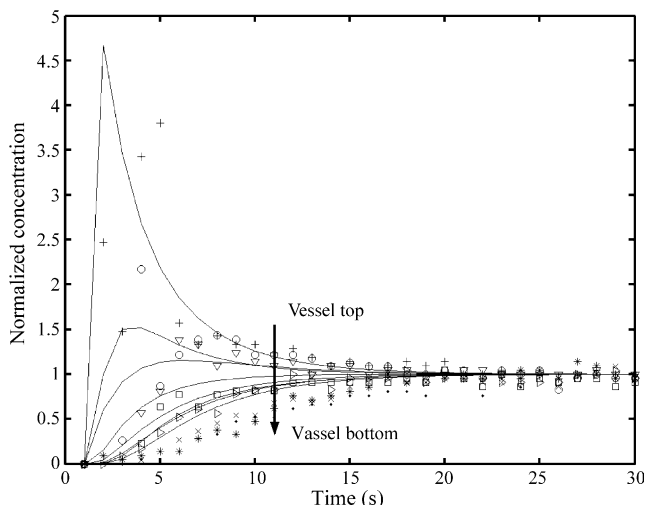


Fig. 6. Comparison of experimental results and simulation results obtained with an RDT6–RDT6 compartment model (simulated values correspond to the continuous lines).

Secondly, the model is limited to two dimensions. Indeed, a three-dimensional model takes into account the tangential component of the mixing action. This aspect will be improved upon in the next section with the inclusion of a tangential flow rate.

At this level, the goal is to translate the CM structure from a deterministic to a probabilistic context. To achieve this, the stochastic Markov chain theory was chosen, because its applicability in mixing processes (to date, especially in the case of particulate mixing processes) has been previously proved [13–15,17,19–22].

The first step is to take the same interconnected compartments network used in the CM. For each compartment (called a state, in the stochastic context), the probabilities of shifting to an adjacent compartment (state) or of staying within the initial compartment (state) were calculated. The flow rates were then translated into probabilities of shifting from one state to another, these probabilities depending on the flow structure (radial or axial) and the ratio of circulating flow on turbulence flow. All the probabilities were collected to con-

struct a transition matrix (Fig. 5), which governs the evolution of the system from a state  $S_i(t)$  to a state  $S_i(t + \Delta t)$  during a transition time  $\Delta t$ . The time taken to achieve a transition is not explicitly given by the model. This important aspect will be studied further in this section.

When having the stochastic model structure derived from CM, the adjustable parameters of the new model must be identified and the estimation method must be elaborated.

The first parameter to estimate is the ratio of the circulation rate on the turbulence rate. This parameter only has an impact on the qualitative results (on the shape of the tracer curves). The  $q_c/q_e$  ratio was calculated for each structure (RDT6, RDT6–RDT6 and RDT6–A315) (Table 2).

On observing the results, it can be seen that the  $q_c/q_e$  ratio is lower when the mixing system comprises an axial flow impeller. These results seem to be in discordance with the general literature covering mixing processes, which recognises axial impellers as high circulation and low turbulence inducing impellers. But the comparison of stirring systems must be performed when operating at the same volumetric power. In our case, the comparison was performed at the same stirrer speed and it was thus normal to obtain a lower value of  $q_c$  when operating with an axial flow impeller.

The second parameter to estimate is the effective duration of a transition  $\Delta t$ . This parameter is very important, since it governs the quantitative result of the simulation and thus the mixing time value. If we look at a simulation (Fig. 7), it can be seen that a given number  $n$  of transitions are necessary before all the states of the models are visited by tracer particles. It thus seems interesting to determine this number  $n$ . This can be easily done by observing the course of a simulation. When running a simulation with a single-staged agitated vessel, five transitions are required before observing the first tracer molecules on the lower part of the vessel. When considering a two-staged stirred vessel, the number of transitions increases to 8 (the concentrations in the last states are very low and cannot be correctly viewed in Fig. 7). We can see from Fig. 7 that the tracer evolution for the RDT6–A315 system exhibits oscillations that are typical of axial flow impellers.

It is important to observe that this number  $n$  does not depend on the operating conditions, but only on the model

Table 2

Calculation of parameters necessary for the shift from a CM to a stochastic model (two-dimensional case)

Impeller(s)	$N$ ( $\text{min}^{-1}$ )	$q_c/q_e$	$k$	$t_{m85\%}$ (s)	$\Delta t$ (s)	$t_c$ (s)
RDT6	230	0.18	32	5	0.15	1.72
RDT6	270	0.16	32	4	0.12	1.47
RDT6	360	0.15	32	3	0.09	1.1
RDT6	450	0.19	32	3	0.09	0.88
RDT6–RDT6	230	0.07	154	14	0.09	1.72
RDT6–RDT6	270	0.07	154	12	0.07	1.47
RDT6–RDT6	360	0.07	154	9	0.05	1.1
RDT6–RDT6	450	0.07	154	8	0.05	0.88
RDT6–A315	230	0.04	133	7	0.05	1.86
RDT6–A315	270	0.03	133	5	0.04	1.59
RDT6–A315	360	0.05	133	5	0.03	1.19
RDT6–A315	450	0.04	133	4	0.026	0.95

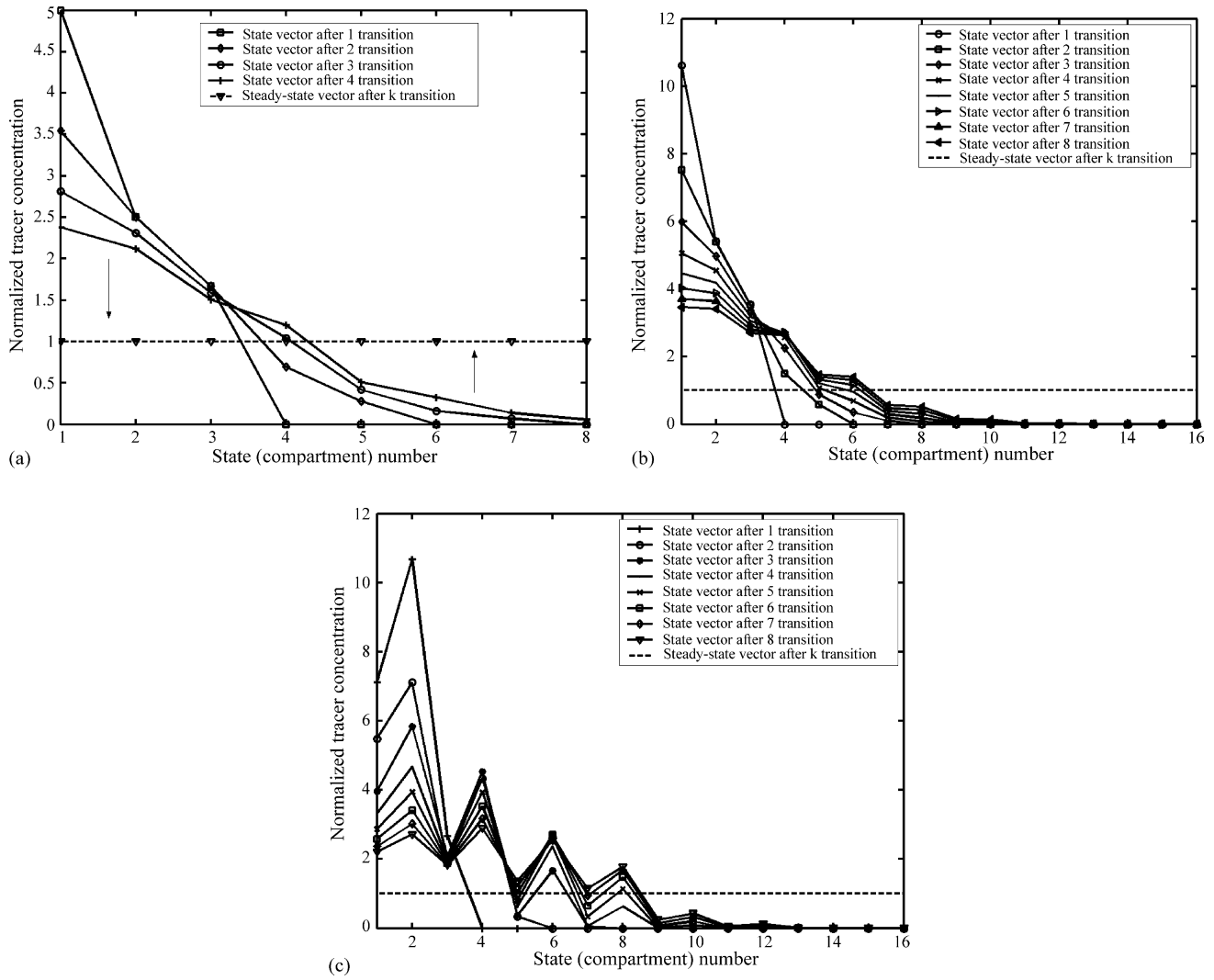


Fig. 7. Repartition of tracer concentrations through the different states of the stochastic model during a simulation (consisting of a series of transitions from state to state). Three impeller systems are presented: (A) RDT6, (B) RDT6–RDT6 and (C) RDT6–A315. The corresponding state number can be found for the RDT6 system in Fig. 4.

structure and the number of states. Thus, for a given geometry and states network,  $n$  will be constant for every operating condition. This number  $n$  will be used further.

The time interval  $\Delta t$  of the stochastic model was determined from experimental data by using the following equation:

$$\Delta t = \frac{t_m}{k} \tag{5}$$

Results of this analysis are presented in Table 2.

To give some physical significance to our model,  $\Delta t$  must be linked to a characteristic time of the mixing process that can be easily calculated by the operator. We chose here the circulation time, which is known to have a strong physical signification for the mixing process. Indeed, Fig. 8 shows that, when increasing the mixing performances and thus when decreasing the circulation time, the parameter  $\Delta t$  drops down to a limiting value, which can be assimilated into the maxi-

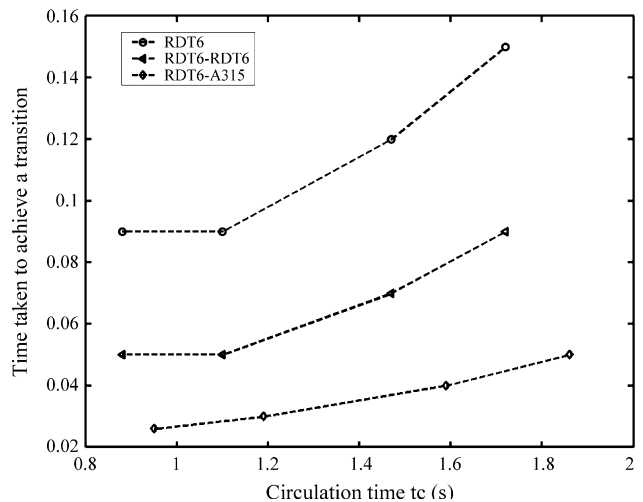


Fig. 8. Evolution of  $\Delta t$  in function of circulation time.

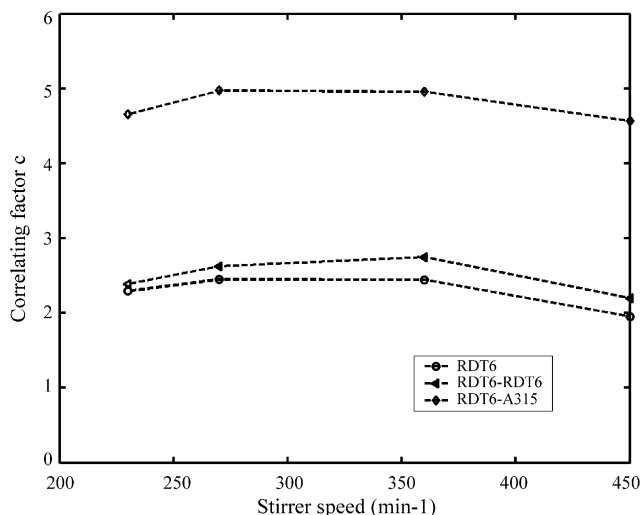


Fig. 9. Evolution of the correlation factor  $c$  involved in Eq. (6) with stirrer speeds for different mixing systems.

imum homogenisation capability of the system. (Looking at Fig. 2, it can be seen that the mixing time values are very low for these operating conditions.) These observations suggest a strong correlation between circulation time and  $\Delta t$ .

In order to extract a correlation from these data, the following equation was considered:

$$\Delta t = \frac{t_c}{n \cdot c} \quad (6)$$

with  $c$  being a correlating factor between  $t_c$  and  $\Delta t$ . The parameter  $n$  corresponds to the number of transitions before all the states (corresponding in practice to the flow regions) are visited by tracer particles. This number of transitions is indeed linked in the physical sense to the circulation time, the circulation process assuming transport of particles throughout the whole volume of the stirred vessel. In Fig. 9, it appears that  $c$  is constant for a given impeller geometry and vessel size. Indeed,  $\Delta t$  must intuitively increase with scale-up and such behaviour can be denoted when comparing the RDT6 and RDT6–RDT6 systems.

Mean values of  $c$  for each stirrer system are compiled in Table 3.

At this stage of the study, it appeared that two parameters needed to be determined in order to run stochastic simulations in the case of mixing in a stirred vessel. The first parameter was the ratio  $q_c/q_e$ , which does not vary significantly for a given stochastic model structure and which only has an impact on the qualitative aspect of the simulation. The second was the time interval, which is the most important parameter.

Table 3  
Mean values of  $c$  (see Eq. (6))

Impeller(s)	$c$	$q_c/q_e$
RDT6	2.28	0.17
RDT6–RDT6	2.49	0.07
RDT6–A315	4.78	0.04

It has been proven that this parameter can be linked to the circulation time by a simple correlation (Eq. (6)).

In the next section, knowledge gained from the two-dimensional model will be extended to a three-dimensional model.

### 3.2. Three-dimensional mixing time experiments

Two-dimensional results obtained in the previous section can be used to quantify the ratio of circulating flow on turbulence-induced flow in each plane of the 3D-version of the model. But in the 3D-model, a third kind of flow, named tangential flow, is necessary to make the connexion between adjacent planes. Tangential flow is responsible for the dispersal of tracer across the different planes of the vessel. Its determination can be made by matching simulations with experimental results. However, we showed, by using a sensitivity analysis, that a  $q_c/q_t$  ratio equal to one leads to better results. Indeed, we also modelled tangential flow by a back-mixing flow. It is thus normal for tangential flows to have values equal to those of turbulence flows, because of the analogy between the two dispersive mechanisms.

Translating the model into a 3D version leads to the modification of some parameters previously defined for the two-dimensional model. The increase in the number of states in the model is traduced by an increase of the  $n$  and  $k$  parameters. Indeed, the value of  $n$  for a single-staged vessel is 8, and 12 for a two-staged vessel. Values of  $k$  can be found in Table 4.

Concerning this table, the same methodology was used to determine the time interval  $\Delta t$  of a simulation in function of the mixing performance of the system (see Eq. (6) previously elaborated for the 2D models).

Fig. 10 presents the evolution of the correlation factor  $c$  in function of stirrer speed for each impeller system tested.

As previously noted for the 2D case, values of  $c$  do not vary significantly for a given impeller system. Mean values of  $c$  are compiled in Table 5.

Eq. (6) and the values of  $c$  reported in Table 5 were used to perform several simulations. Fig. 11 shows a comparison

Table 4  
Calculation of the parameters involved in stochastic models (three-dimensional case)

Impeller(s)	$N$ (min <sup>-1</sup> )	$q_c/q_e$	$q_t/q_e$	$k$	$t_{m85\%}$ (s)	$\Delta t$ (s)
RDT6	230	0.18	1	80	5	0.062
RDT6	270	0.16	1	80	4	0.05
RDT6	360	0.15	1	80	3	0.037
RDT6	450	0.19	1	80	3	0.037
RDT6–RDT6	230	0.07	1	292	16	0.054
RDT6–RDT6	270	0.07	1	292	14	0.047
RDT6–RDT6	360	0.07	1	292	12	0.041
RDT6–RDT6	450	0.07	1	292	10	0.034
RDT6–A315	230	0.04	1	290	12	0.041
RDT6–A315	270	0.03	1	290	10	0.034
RDT6–A315	360	0.05	1	290	10	0.034
RDT6–A315	450	0.04	1	290	8	0.027



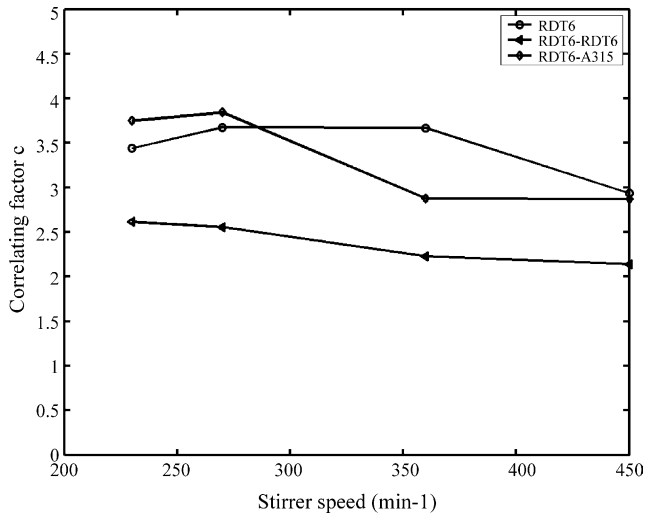


Fig. 10. Evolution of the correlation factor  $c$  involved in Eq. (6) with stirrer speed for different mixing systems (three-dimensional system).

Table 5  
Mean values of  $c$  for a 3D-model (see Eq. (6))

Impeller(s)	$c$
RDT6	3.42
RDT6–RDT6	2.38
RDT6–A315	3.33

of these simulations with experimental results. It can be seen that the proposed parameter evaluation methodology led to acceptable results.

### 3.3. Residence time distribution experiments

In order to perform RTD simulations, the 3D-model must be adapted by adding an additional state, named the absorbing state. This state is responsible of the absorption of tracer molecules and represents the lower zone of the vessel, including the liquid evacuation hole. The transition matrix (Fig. 5) must be adapted to contain the absorbing state and has the aspect shown in Fig. 12 [19].

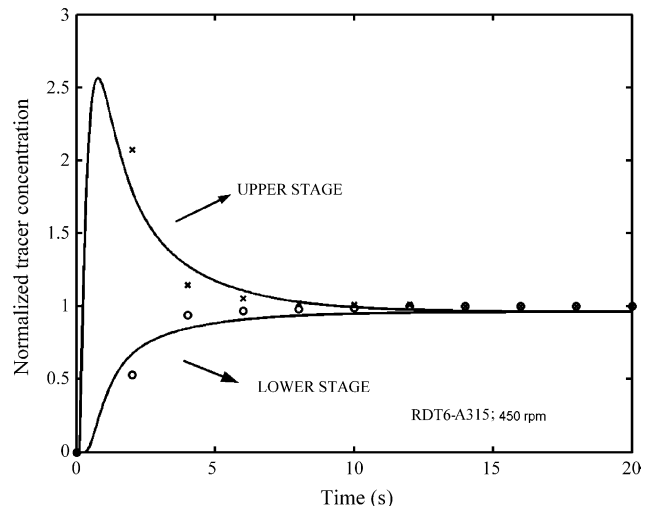
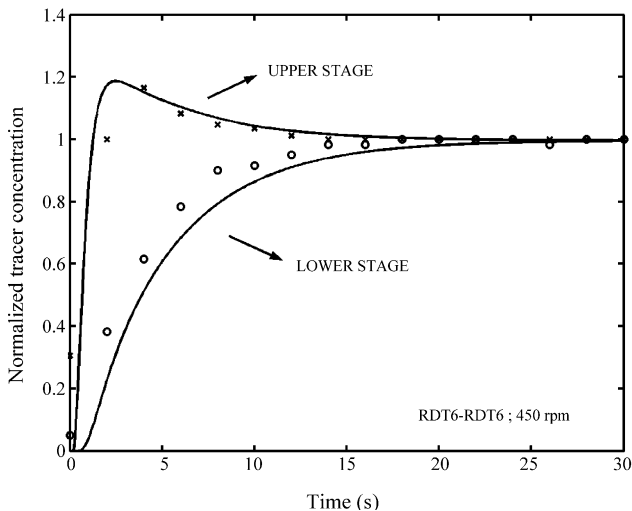
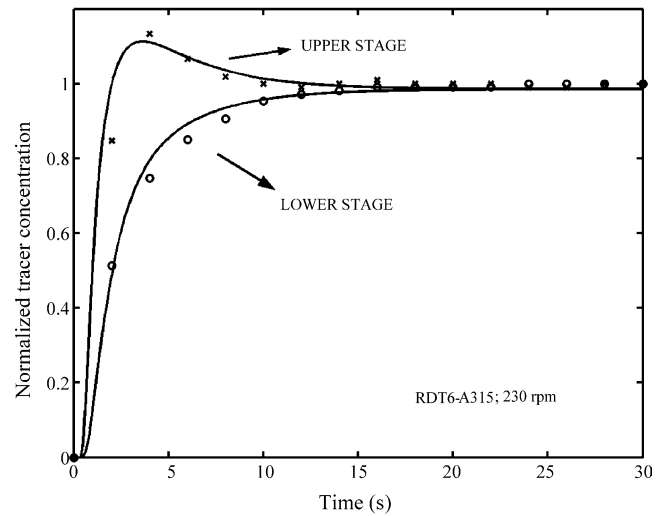
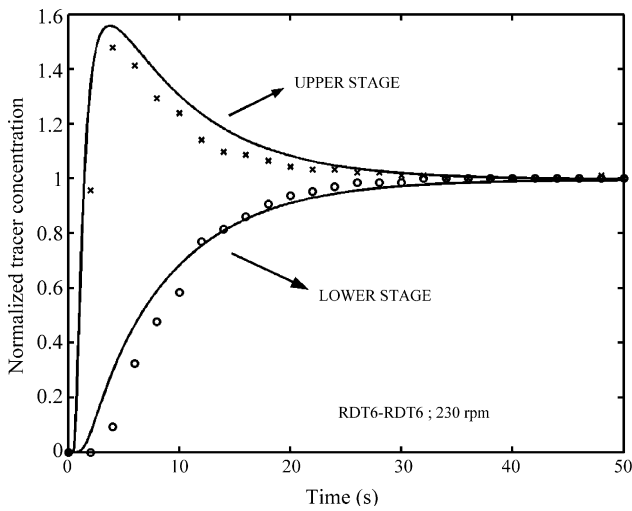


Fig. 11. Comparison between experimental (dot) and simulated results (line) with three-dimensional stochastic models.

$$\begin{bmatrix} T_{batch} & B \\ 0 & 1 \end{bmatrix}$$

Fig. 12. Transition matrix containing an absorbing state used to perform RTD simulations.

In this matrix,  $T_{batch}$  is the transition matrix previously presented in Fig. 5;  $B$  is a column vector containing zero elements and a single element containing  $q_{exit}$ ;  $0$  is a line vector containing zero elements and  $1$  is a unit element responsible for the absorbing process.

In this case, an additional parameter expressing the liquid flow rate leaving the system must be determined. This flow is experimentally known and its determination does not cause any difficulties.

At this stage, it is thus possible to perform simulations by entering the previously determined parameters of the model. In this section, we will perform simulations and compare the results with experimental data. Examples of the quality of the simulations can be viewed in Fig. 13.

These simulations were performed by using parameters ( $q_c$ ,  $q_e$ ,  $q_t$  and  $\Delta t$ ) coming from three-dimensional mixing experiments (see Tables 4 and 5). The simulations improved the validity of these parameters for the mixing systems considered.

### 3.4. Stochastic simulation of particle circulation in a stirred vessel

Another interesting property of the stochastic model is that the transition matrix  $T$  can be directly used to perform single particle circulation simulations. Indeed, the  $T$  matrix contains all the transition probabilities from state to state and these probabilities can be used in conjunction with a random number generator to provide the path taken by a particle in

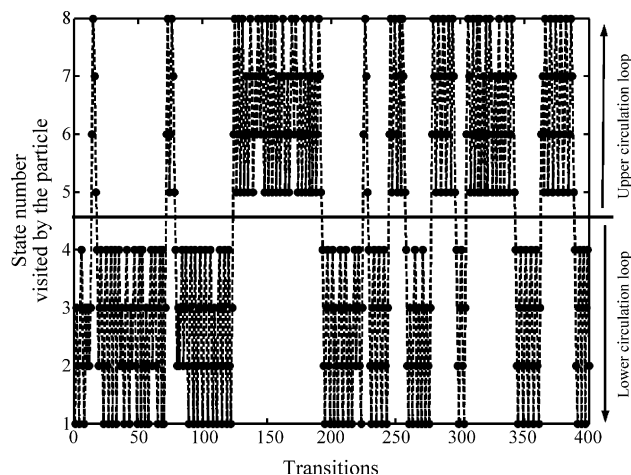


Fig. 14. Stochastic simulation of a particle circulation inside a stirred vessel. The arrangement of states corresponds to the axial “basic plane” defined in Fig. 3.

displacement inside the stirred vessel. In a bioprocess context, it is very important to know the passage frequency of the micro-organisms in some crucial flow regions of the bioreactor (for example, the substrate addition point in the case of a fed-batch culture, which can cause a stress due to the high concentration levels). In the case of a circulation process simulation, only the axial planes of the vessel are important. We can thus limit our observations by using only one of the basic planes of the three-dimensional model defined in Fig. 3. An example of particle travel from state to state is given in Fig. 14.

These results can be exploited to calculate the passage frequency of a particle inside a given state and, in this way, the circulation time in relation with this state. When simulation involves a lot of transitions, circulation time distribution can be established for a given state or a given set of states. Such an example is given in Fig. 14 for 200,000 transitions, which

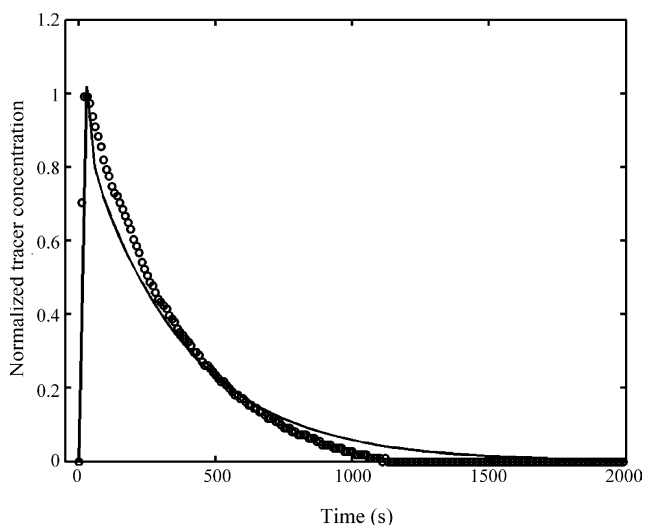
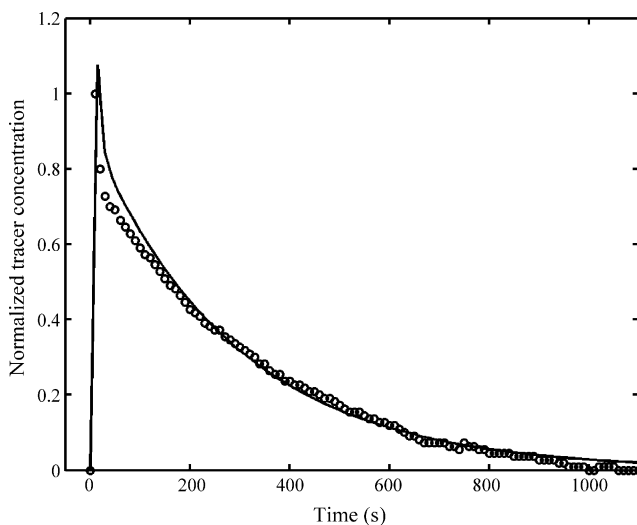


Fig. 13. Comparison between experimental (dot) and simulated RTD results (line). Right: RDT6–A315 system; left: RDT6–RDT6 system.

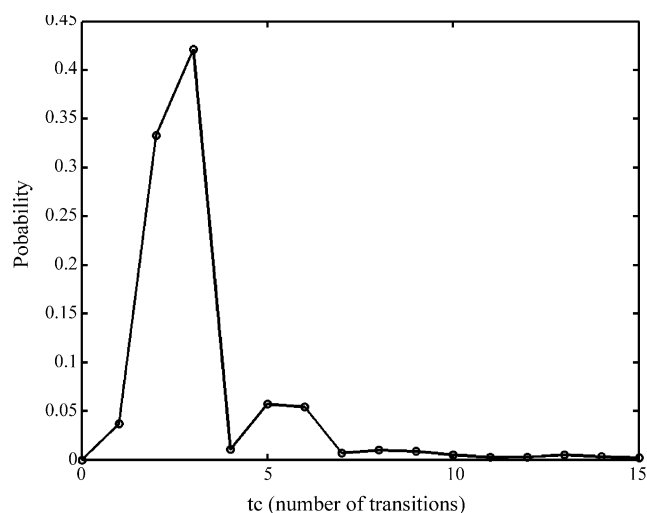


Fig. 15. Circulation time distribution related to a given state of the stochastic model (circulation time  $t_c$  is not expressed here in seconds but in number of transitions).

correspond more or less to 2300 circulations through a particular state. The state chosen here corresponds to the flow region located at the top of the vessel, which, in case of a fed-batch bioprocess, is subject to substrate pulse addition. This in turn can affect cellular metabolism. An important fact is that the circulation time distribution (CTD), represented in Fig. 15, exhibits a log-normal shape, as described in the literature [16].

The maximum of probability corresponds to three transitions before returning to the specified state and is in accordance with the basic plane structure of the model, which involves four states per circulation loop. This phenomenon can also be viewed in Fig. 14, which highlights the presence of two circulation loops in the axial plane of the vessel. The variance comes from the fact that the particle can bypass the circulation loop constituted by a set of four states. The variance can be increased by considering several concentric circulation loops, but this requires a modification of the model structure. This important fact, as well as the extensive development of the circulation aspect, emerges from the objectives of this publication and would need a separate study.

#### 4. Conclusion

A methodology has been presented here aimed at facilitating the calculation of the parameters of stochastic models. It involves the use of estimated flow rates coming from compartment mixing model analysis. The ratio between these flow rates can be assumed to be constant for a given impeller system, which greatly facilitates the elaboration of the transition matrix. A second important parameter to determine is the time interval  $\Delta t$ , necessary to achieve a simulation step. This time step is not explicitly given by the model but, after appropriate analysis, it appears that a simple correlation could be used to

make the connexion between a simulation step and a real time interval ( $\Delta t$ ). The correlation (Eq. (6)) contains an adjustable parameter, which depends only on the impeller geometry, in the range of operating conditions tested. Corresponding values of  $c$  can be found in Table 3 for two-dimensional models and in Table 5 for three-dimensional ones.

The stochastic model can be used for model mixing behaviour of different impeller systems in stirred vessels, resolution being equivalent with that obtained with classical CM. Indeed, simulation performances were similar for each kind of model investigated in this study. This equivalency allows the application of the stochastic model to the study of mixing in fluid systems. This approach is interesting because of the exclusive properties of the stochastic model (not found in the classical CM), which can be used to investigate special mixing behaviour in the process industry. The aim of our study was to combine a structured hydrodynamic model (such as CM or more recently the stochastic model) with microbial kinetics. In this area, the exposure of micro-organisms to gradients can be investigated by performing particle-tracking simulations. These simulations can be simply performed by using the transition matrix of the model, as shown in this study. A second advantage of the stochastic model in this area comes from the discrete evolution of the system during a simulation run. Indeed, this characteristic of the stochastic model allows the calculation of a given state by using Eq. (3) ( $S_i = T^i \cdot S_0$ ). This property can be exploited when dealing with complex models involving reactor hydrodynamics and reacting species (such as micro-organisms in the presence of a nutrient), which require a large amount of computational time and space [23].

#### References

- [1] P. Vrabel, R.G.J.M. van der Lans, F.N. van der Schot, K.Ch.A.M. Luyben, B. Xu, S.O. Enfors, CMA: integration of fluid dynamics and microbial kinetics in modelling of large-scale fermentations, *Chem. Eng. J.* 84 (2001) 463–474.
- [2] D. Vlaev, R. Mann, V. Lossev, S.D. Vlaev, J. Zahradnik, P. Seichter, Macro-mixing and *Streptomyces fradiae*: modelling oxygen and nutrient segregation in an industrial bioreactor, *Trans. IChemE* 78 (2000) 354–362.
- [3] J. Zahradnik, R. Mann, M. Fialova, D. Vlaev, S.D. Vlaev, V. Lossev, P. Seichter, A network-of-zones analysis of mixing and mass transfer in three industrial bioreactors, *Chem. Eng. Sci.* 56 (2001) 485–492.
- [4] Y.Q. Cui, R.G.J.M. van der Lans, H.J. Noorman, K.Ch.A.M. Luyben, Compartment mixing model for stirred reactors with multiple impellers, *Trans. IChemE* 74 (1996) 261–271.
- [5] V. Machon, M. Jahoda, Liquid homogenization in aerated multi-impeller stirred vessel, *Chem. Eng. Technol.* 23 (2000) 869–876.
- [6] B. Mayr, P. Horvat, E. Nagy, A. Moser, Mixing models applied to industrial batch reactor, *Bioprocess Eng.* 9 (1993) 1–12.
- [7] B. Mayr, E. Nagy, P. Horvat, A. Moser, Scale-up on basis of structured mixing models: a new concept, *Biotechnol. Bioeng.* 43 (1994) 195–206.
- [8] J.M.T. Vasconcelos, S.S. Alves, A.W. Nienow, W. Bujalski, Scale-up of mixing in gassed multi-turbine agitated vessels, *Can. J. Chem. Eng.* 76 (1998) 398–404.

- [9] J.M.T. Vasconcelos, S.S. Alves, J.M. Barata, Mixing in gas–liquid contactors agitated by multiple turbines, *Chem. Eng. Sci.* 50 (1995) 2343–2354.
- [10] P. Vrabel, R.G.J.M. van der Lans, K.Ch.A.M. Luyben, L. Boon, A.N. Nienow, Mixing in large-scale vessels stirred with multiple radial or radial and axial up-pumping impellers: modelling and measurements, *Chem. Eng. Sci.* 55 (2000) 5881–5896.
- [11] R. Mann, S.K. Pillai, A.M. El-Hamouz, P. Ying, A. Togatorop, R.B. Edwards, Computational fluid mixing for stirred vessels: progress from seeing to believing, *Chem. Eng. J.* 59 (1995) 39–50.
- [12] R. Mann, D. Vlaev, V. Lossev, S.D. Vlaev, J. Zahradnik, P. Seichter, A network-of-zones analysis of the fundamentals of gas–liquid mixing in an industrial stirred bioreactor, *Récents progrès en génie des procédés* 11 (52) (1997) 223–230.
- [13] W. Pippel, G. Philipp, Utilization of Markov chains for simulation of dynamics of chemical systems, *Chem. Eng. Sci.* 32 (1977) 543–549.
- [14] M. Rubinovitch, U. Mann, Single-particle approach for analyzing flow systems. Part I: visits to flow regions, *AIChE J.* 29 (4) (1983) 658–662.
- [15] L.T. Fan, L.S. Fan, R.F. Nassar, A stochastic model of the unsteady state age distribution in a flow system, *Chem. Eng. Sci.* 34 (1979) 1172–1174.
- [16] P.K. Namdev, B.G. Thompson, M.R. Gray, Effect of feed zone in fed-batch fermentations of *Saccharomyces cerevisiae*, *Biotechnol. Bioeng.* 40 (2) (1992) 235–246.
- [17] T. Howes, M. Brannock, G. Corre, Development of simplified flow models from CFD simulations, in: Third International Conference on CFD in the Minerals and Process Industries, CSIRO, Melbourne, Australia, 2003.
- [18] B. Mayr, P. Horvat, A. Moser, Engineering approach to mixing quantification in bioreactors, *Bioprocess Eng.* 8 (1992) 137–143.
- [19] H. Berthiaux, J. Dodds, Modeling classifier networks by Markov chains, *Powder Technol.* 105 (1999) 266–273.
- [20] M. Rubinovitch, U. Mann, A single particle approach for analysing flow systems. Part II: regional residence times and local flow rates, *AIChE J.* 29 (4) (1983) 663–668.
- [21] M. Rubinovitch, U. Mann, A single particle approach for analysing flow systems. Part III: multiple fluids, *AIChE J.* 31 (4) (1985) 615–620.
- [22] J. Szépvölgyi, E. Diaz, J. Gyenis, New stochastic modelling of mixing in process operations, *Chem. Eng. Process.* 38 (1999) 1–9.
- [23] F. Delvigne, T. El Mejdoub, J. Destain, J.M. Delroisse, M. Vandenberg, E. Haubruge, P. Thonart, Estimation of bioreactor efficiency through structured hydrodynamic modelling: case study of a *Pichia pastoris* fed-batch process, *Appl. Biochem. Biotechnol.* 121–124 (2005) 653–671.